AD-A190 647 UNIVERSITY RESEARCH INSTRUMENTATION PROGRAM EQUIPMENT FOR INSTRUMENTATION..(U) MARYLAND UNIV COLLEGE PARK DEPT OF CIVIL ENGINEERING D J GOODINGS ET AL. 1/1

UNCLASSIFIED 23 NOV 87 AFOSR-TR-87-1990 AFOSR-86-0333 F/G 14/2 NL

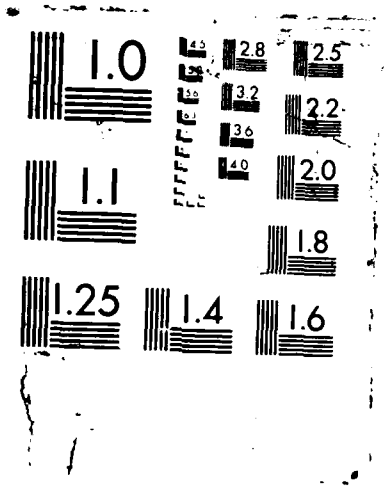
1.0
1.1
1.25
1.4
1.6
1.8
2.0
2.2
2.5
2.8
3.2
3.6
4.0

Unclassified
CLASSIFICATION OF THIS PAGE

(2)

MENTATION PAGE

1a. REPORT SECURITY: Unc	1b. RESTRICTIVE MARKINGS: DTIC FILE COPY
2a. SECURITY CLASSI: **AD-A190 647**	3. DISTRIBUTION/AVAILABILITY OF REPORT: Approved for public release; distribution is unlimited.
2b. DECLASSIFICATION/DOWNGRADING SCHEDULE	
4. PERFORMING ORGANIZATION REPORT NUMBER(S)	5. MONITORING ORGANIZATION REPORT NUMBER(S): AFOSR-TR- 87-1990
6a. NAME OF PERFORMING ORGANIZATION: UNIV. OF MARYLAND D.J. Goodings and B. Ayyub	6b. OFFICE SYMBOL (If applicable):
6c. ADDRESS (City, State, and ZIP Code): Dept. of Civil Engineering, University of Maryland, College Park, MD 20742	7a. NAME OF MONITORING ORGANIZATION: AFOSR/NA
	7b. ADDRESS (City, State, and ZIP Code): Bolling AFB BLDG 410, Washington DC 20332-6448
8a. NAME OF FUNDING/SPONSORING ORGANIZATION: AFOSR/NA	8b. OFFICE SYMBOL (If applicable): NA
8c. ADDRESS (City, State, and ZIP Code): Bolling Air Force Base BLDG 410, Washington, DC 20332-6448	9. PROCUREMENT INSTRUMENT IDENTIFICATION NUMBER: AFOSR-86-0333
	10. SOURCE OF FUNDING NUMBERS: PROGRAM ELEMENT NO. 61102 F; PROJECT NO. 2917; TASK NO. A1; WORK UNIT ACCESSION NO.

11. TITLE (Include Security Classification)
Equipment Grant - Bridge Rehabilitation and Geotechnical Explosives Testing

12. PERSONAL AUTHOR(S)
D.J. Goodings and B. Ayyub

13a. TYPE OF REPORT	13b. TIME COVERED	14. DATE OF REPORT (Year, Month, Day)	15. PAGE COUNT
Final	FROM Aug. 86 TO Sept. 87	87-11-23	32

16. SUPPLEMENTARY NOTATION

17. COSATI CODES			18. SUBJECT TERMS (Continue on reverse if necessary and identify by block number)
FIELD	GROUP	SUB-GROUP	Data Acquisition System

19. ABSTRACT (Continue on reverse if necessary and identify by block number)

The report describes the performance criteria sought and the system selected for data acquisition on two quite different civil engineering research facilities: one for testing composite structural section with application to bridge rehabilitation, and one for geotechnical centrifugal modelling. It also outlines the initial applications of the system.

20. DISTRIBUTION/AVAILABILITY OF ABSTRACT	21. ABSTRACT SECURITY CLASSIFICATION	
☒ UNCLASSIFIED/UNLIMITED ☐ SAME AS RPT ☐ DTIC USERS	Unclassified	
22a. NAME OF RESPONSIBLE INDIVIDUAL: Spencer T. Wu	22b. TELEPHONE (Include Area Code): (202) 767-6962	22c. OFFICE SYMBOL: AFOSR/NA

DD FORM 1473, 84 MAR — 83 APR edition may be used until exhausted. All other editions are obsolete.

SECURITY CLASSIFICATION OF THIS PAGE
Unclassified

Department of Defense

University Research Instrumentation Program

FY 1986/1987

Equipment for Instrumentation of

Bridge Rehabilitation

and Geotechnical

Explosives Testing

D.J. Goodings and B. Ayyub
Department of Civil Engineering
University of Maryland
College Park, Maryland 20742

Final Report
AFOSR - 86-0333 (UM 01-5-28143)
Equipment Grant for Instrumentation
of Bridge Rehabilitation and Geotechnical
Explosives Testing

A high speed, high resolution data acquisition, signal conditioning and data storage system was purchased over the duration of this equipment grant. It has been applied directly to two federally funded research projects, one involving analysis of prestressed composite steel beams for the strengthening and rehabilitation of bridges, and one involving modelling of explosion induced craters in sand using the geotechnical centrifuge. Its selection, however, was based on its versatility for application to these as well as a host of as yet undetermined future laboratory situations. This report outlines these items in detail.

I. The System

The data acquisition system for this equipment grant was designed to be versatile and to provide high speed data acquisition, signal conditioning, and storage. It was required to be capable of connection with strain gauges, pressure, displacement and passive transducers, temperature detectors, thermocouples, load cells and flow metres. It was also important that it be easy to move and to interface with existing and future research equipment in the engineering laboratory.

The system selected is manufactured by Optim Electronics. Other auxiliary pieces of equipment in keeping with the objectives of the grant were purchased from Hewlett-Packard, Sangamo, Sperry Corporation, and Druck Inc. A list of the specific items purchased and their sources is given below; the item numbers are consistent with those of the original proposal.

Item No.	Item	Quantity	Source
1 and 2	Main Data Acquisition, Control, Storage Unit	2	Optim
3	Analog Input Module	5	Optim
4	Analog Input Module	3	Optim
5	Voltage Energization Module	1	Optim
6	Current Energization Module	8	Optim
7	Channel Terminal Boxes	9	Optim
8	IBM-AT Host Computer System	3	Computer Emporium
9	Graphics Plotter	2	Hewlett-Packard
10	User Software	1	Optim
11	4-Channels Signal Conditioner	1	Sangamo
12	Displacement Transducers	4	Sangamo
13	Analog Accustor Electronic Clinometer	6	Sperry Corp.
14	HP Dual Output + 0-25 VDC Power Supply	1	L.A. Benson
15	Pressure Transducers	6	Druck Inc.
16	Security Truck (Cabinet)	1	L.A. Benson
17	Security Cables	-	University of Md.

The following companies provided the equipment:

Item No.	Source	Name of Contact	Address & Telephone No.
1 to 7, 10	OPTIM Electronics	Roger Moore	Middlebrook Tech Park 1240 Middlebrook Rd. Germantown, MD 10784 (301) 428-7200
8	Computer Emporium Univ. of Md. IBM	Joan Kessner	Computer Court Bldg. 339 Rm 1400, Univ. of Md. College Park, MD 20742 (301)454-5825
9,14	Hewlett-Packard	Azita Moghaddan	2 Choke Cherry Rd. Rockville, MD 20850 (301)362-7625
11,12	Sangamo Transducer	Robert Anderson	1875 Grand Island Blvd. Grand Island, NY 14072 (716) 773-0090
13	Sperry Corporation Aerospace and Marine Group	Nicole	Sensing System-MSDV-2 PO Box 21111 Phoenix, AZ 85036-1111 (800)545-3243
15	Druck Inc.	B. King	Miry Brook Road Danbury, CT 06810 (203) 792-8981
16	L.A. Benson Co.	None	PO Box 2137 Baltimore, MD 21203 (800) 492-0277
17	University of Md.		Dept. of Civil Engineering University of Maryland College Park, MD 20742 (301) 454-2438

All items have been received. Optim Electronics is continuing to provide training and back-up assistance in operating the software.

II. Application

A. Bridge Rehabilitation -

The first application is to two projects funded by the National Science Foundation. The projects address the question of how to strengthen and rehabilitate girders of existing bridges by prestressing the existing structural steel sections, an economical, effective and fast way to ensure efficient land transportation. The scope of the problem is evident when one considers that over one-half of the approximately 600,000 highway bridges in the United States are over 30 years old, and each year on average, 12,000 will reach the end of their 50 year design life. The first phase of the project is determining both the strength characteristics and the reliability of upgraded and retrofitted composite steel girders, including examination of bonded and unbonded tendons. The second phase is to assess the strength of those composite steel girders under long term repeated loadings. Specifically, the OPTIM data acquisition system 2200 was used to test eight prestressed composite steel/concrete girders and five components of bridge decks with welded steel mesh. It was selected because of its ability to scan often and record data from many types of instrumentation, including strain gages LVDT's clinometers and load cells. The role of the data acquisition system in this research is to speed record information measured by the experimental instrumentation, so that more information can be recorded than is presently possible by virtue of its rapid scanning feature, and to store it in a form which can be easily accessed for analysis. In the following section, a description is given about the flexure test of bridge decks and sample listings of transducer description, transducer calibration, experiment table and measurements.

The loading, placement of strain gages, deflection gages, and rotation gage are shown in Figures 1 to 4. The specimen had four strain gages at the top of the concrete to measure the extreme compressive force, four concrete strain gages impeded inside the slab to measure the strain of the concrete at the level of the steel, three strain gages placed in the top reinforcing steel to measure the compressive strain in the compression steel, and four strain gages on the bottom reinforcing steel to measure the tensile strain in the tensile steel. The deflection was measured with two deflection gages (LVDT's) at the centerline of the slabs, and the rotation was measured with an electronic clinometer placed at the support. A typical test specimen cross-sectional area is shown in Figure 1.

Because of the tremendous amount of data measurement needed, the OPTIM optilog data acquisition system was used which is driven and controlled by optilog opus 2000. The optilog has extensive measurement capabilities which enables it to obtain many scans of data from strain gages, LVDT's, clinometers, and load cells in a significantly short time. For each loading increment, all the instrumentation measurements were scanned at least 100 times and stored on the hard disk of an IBM AT. The average of these readings produces one reading for the particular instrument. Appendix 1 gives further information on the sensors, the experiments, the transducer calibration and the measurements taken, in the form of output from the system.

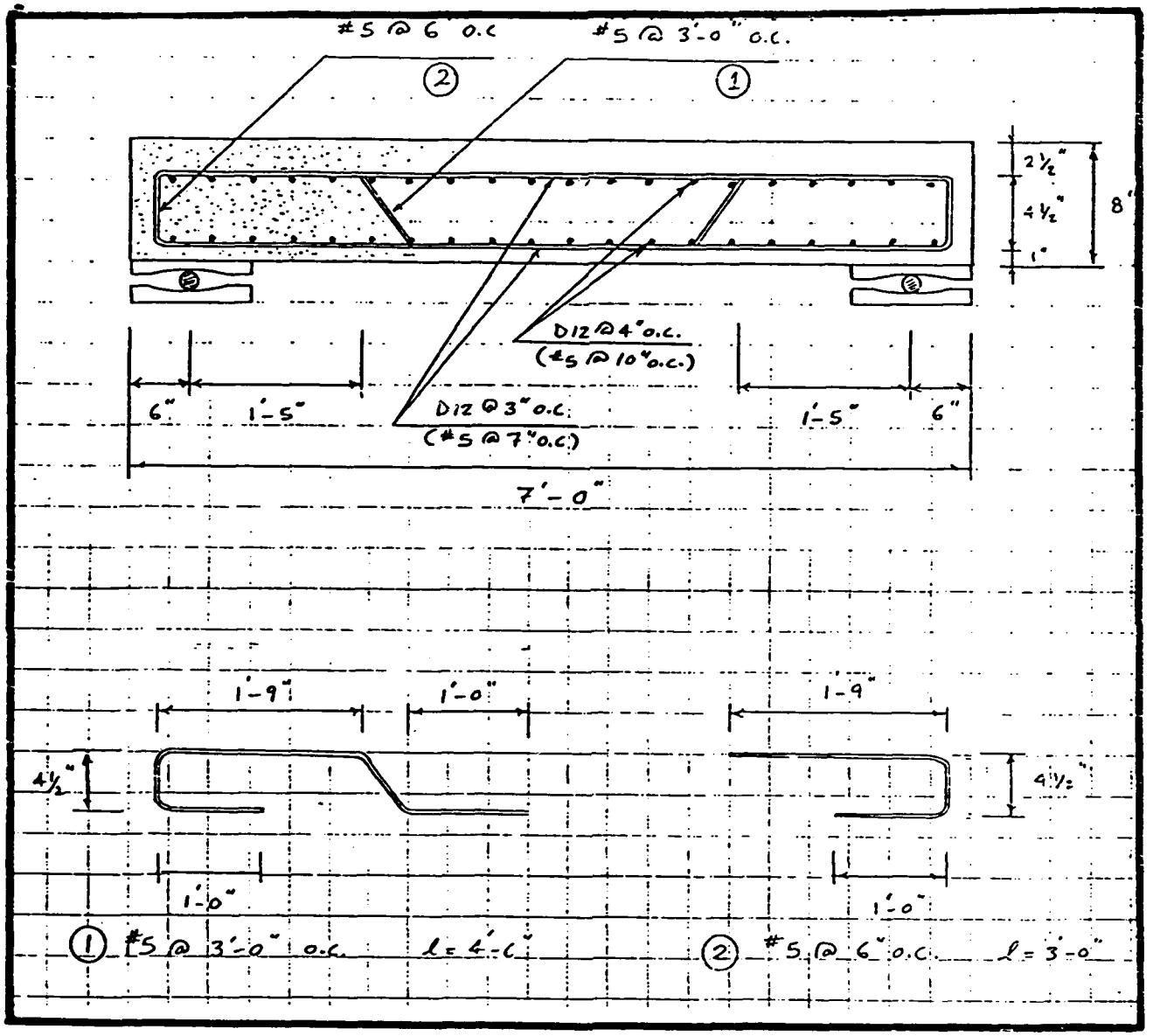

Figure 1 Details and Dimensions of Flexural Slab Specimen

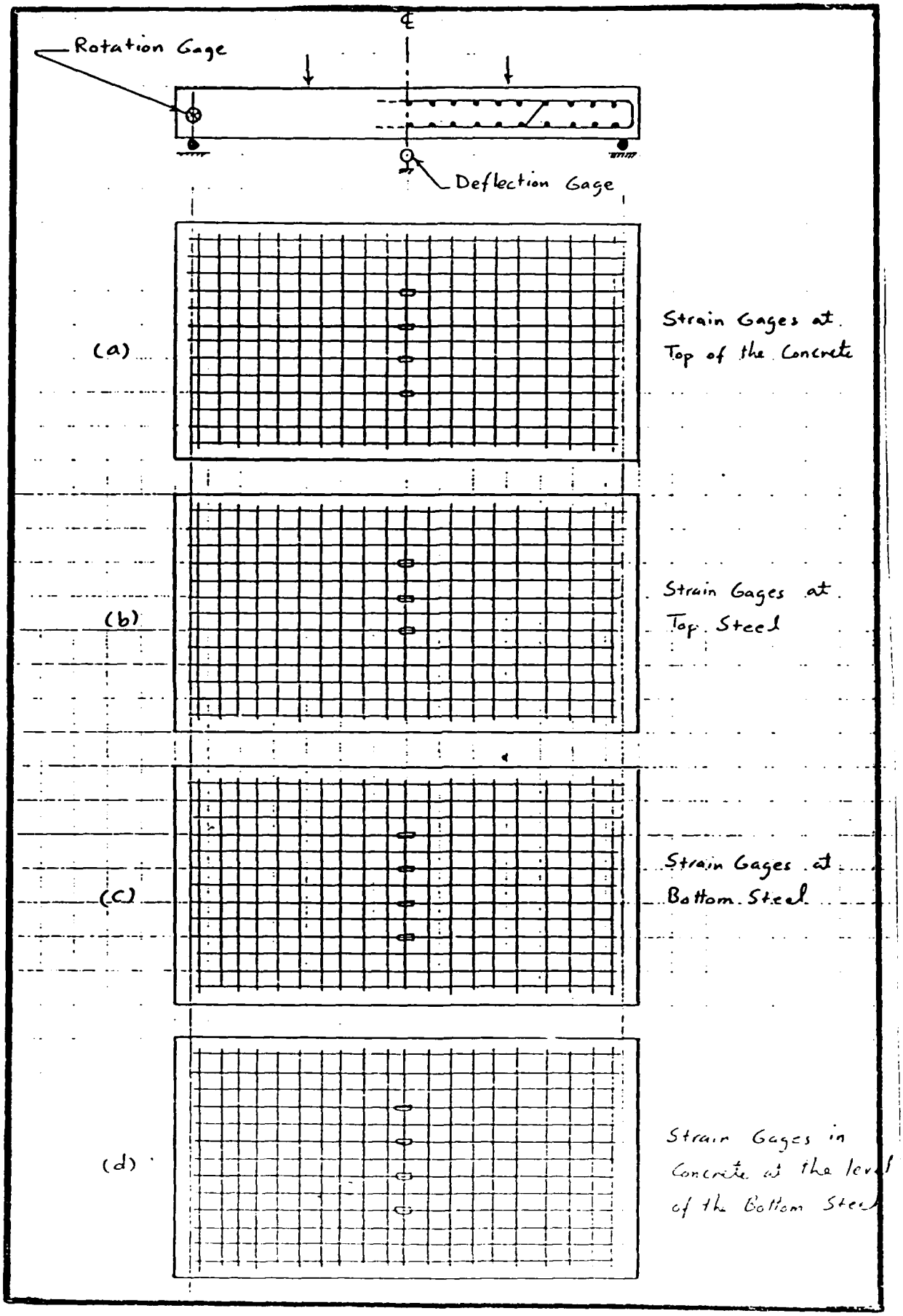

Figure 2 Loading, Placement of Strain Gages, Deflection Gages, and Rotation Gage

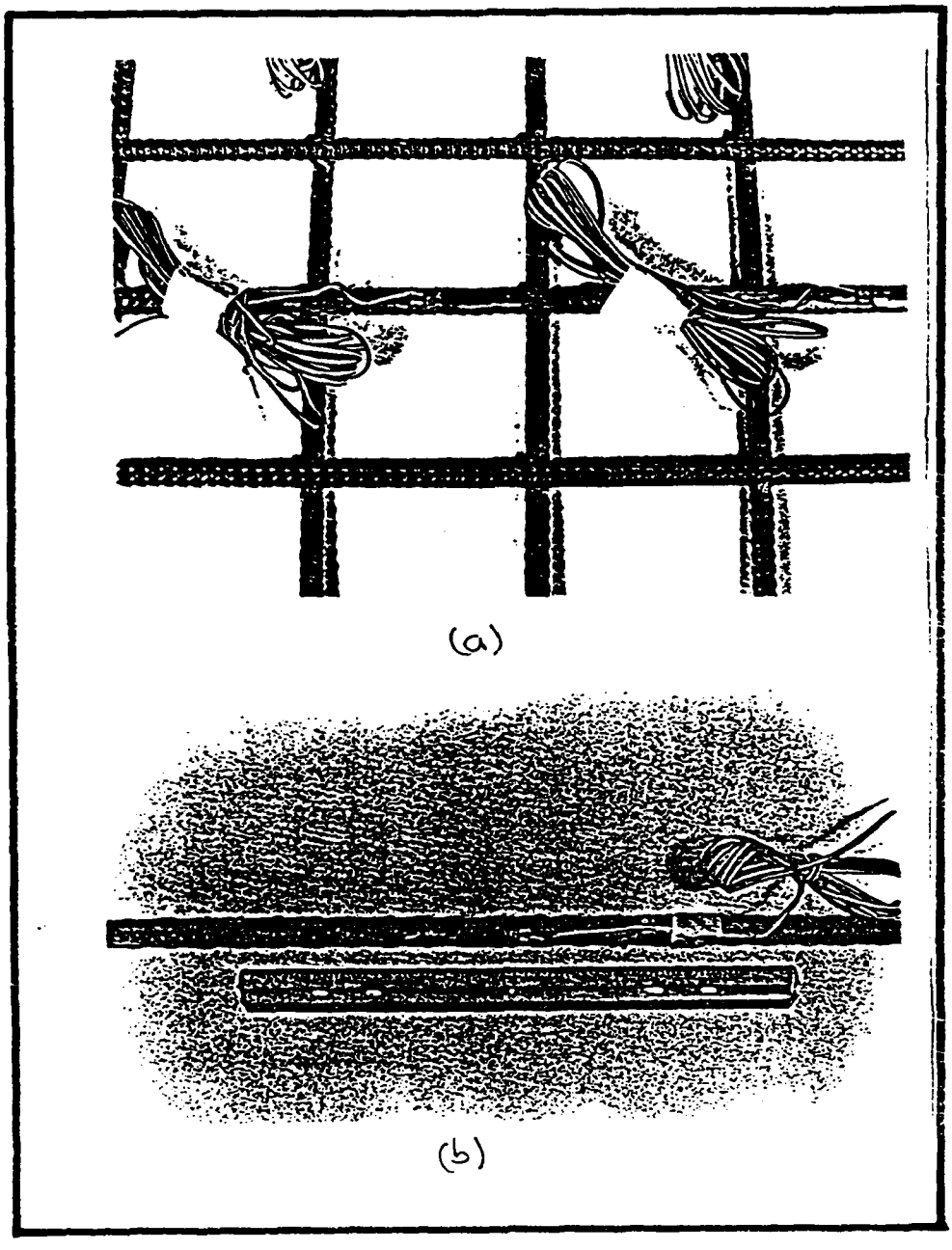

Figure 3 Reinforcing Steel Strain Gages
(a) Welded Steel Mesh Strain Gages
(b) Conventional Reinforcement Strain Gages

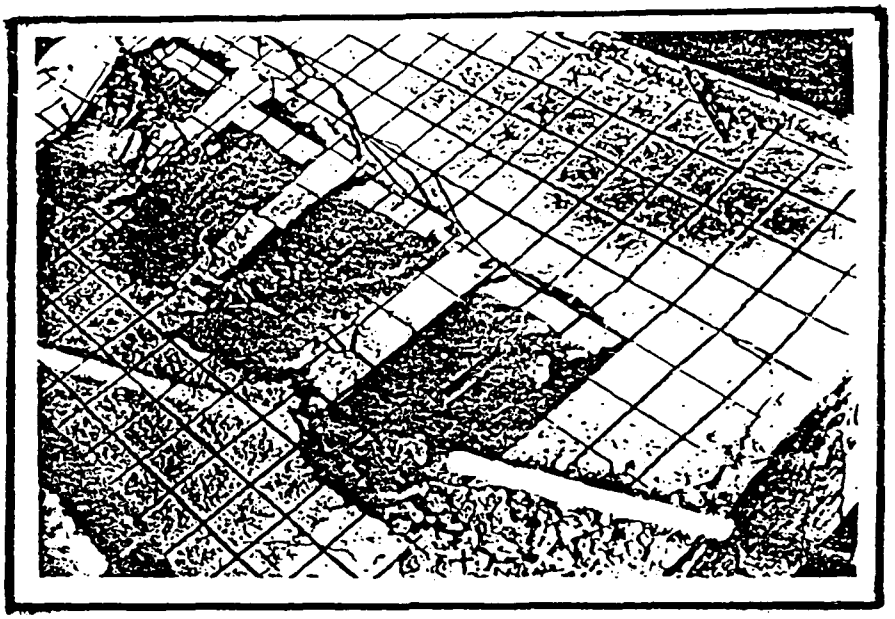

(a)

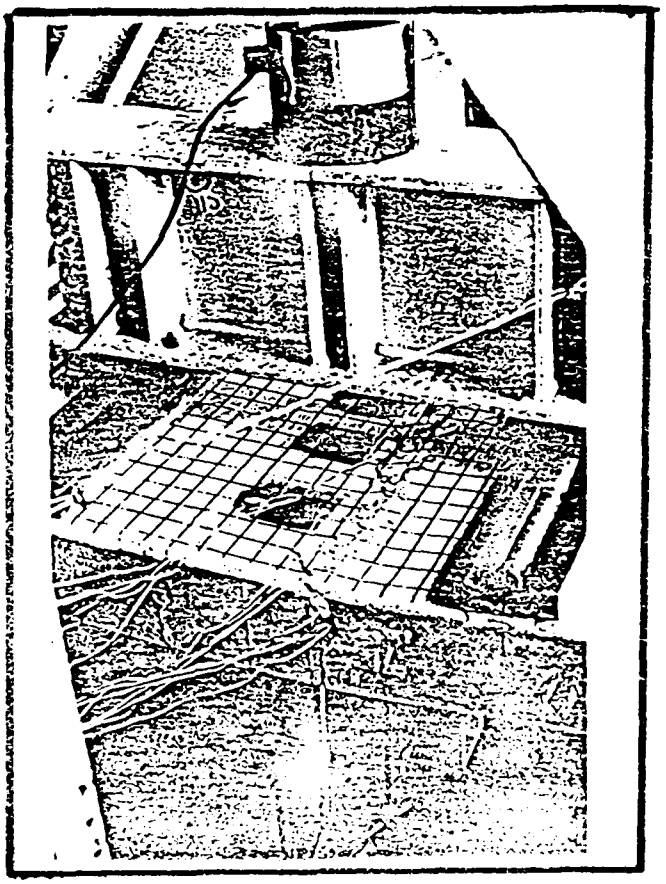

(b)

Figure 4 Use of the Concrete Strain Gages
(a) strain gages with protection coating
(b) strain gages with mechanical protection

B. Geotechnical -

The second application is to a project funded by the Air Force Office of Scientific Research involving geotechnical centrifuge modelling of craters caused by large explosives in dry sand. It is clear in examining field data of dimensions of full scale craters that there exists enormous scatter, so large that reasonable predictions of crater size by either theory or interpolation of existing data has not been possible. Geotechnical centrifuge modelling conducted in high speed centrifuges at over 300g has proven itself recently to be an invaluable technique in studying such events in a controlled and repeatable laboratory environment. Verification of the technique, particularly of the absence of scaling effects, in the intermediate range of centrifugal accelerations more typically available in geotechnical centrifuges at universities had not been addressed. In AFOSR-86-0095, we are examining just that with respect to acceleration and particle size effects between 1g and 100g. The role of the data acquisition system in this research has been to process data recovered after the test, since there have been to date no commerically available high speed stress cells capable of measuring stress waves during the test explosion.

Figures 1 and 2, and Table 1 in the paper attached in Appendix 2 submitted to and accepted for the first international conference dedicated to geotechnical centrifuge research are examples of how the system has been applied for this first project. Table 1 lists model test data. Raw data were taken from the models to achieve four complete cross-sections of each crater produced by detonation of an explosive. The shapes of the full cross-sections of a given crater were then averaged to achieve a single average half cross-section, and the volume was calculated by means of cylindrical shells. The data acquisition system was used in these simple but tedious calculations. The system was then used to examine correlation between different model parameters. Figure 1 relates two dimensionless Buckingham π groups, one reflecting explosive weight and model scale, and the other reflecting crater volume; the data fit was very satisfactory for an arbitrarily selected 80% confidence interval. Figure 2 relates data of this research to data of models tested by two other authors, Schmidt and Holsapple; field data of craters from four full scale events are also shown. Whereas the field data could be directly plotted, Schmidt and Holsapple's data required manipulation to plot on the same Figure. This manipulation was also conducted using the data acquisition system.

We are also in the process of applying the system to a jointly funded Federal Highway Administration and Maryland State Highway Administration project involving centrifugal modelling of the behaviour of geotextile reinforced clay walls, and to a second project to examine changes in flow regime in high speed seepage through granular soils in a permeameter on the centrifuge. In the case of the jointly funded highway project, the measurement taken will be displacements read by linear voltage displacement transducers. The data will be collected and stored by the system for later manipulation. In the case of the seepage project, temperature and water pressures will be measured with transducers in flight, to examine effects of acceleration on soil permeability; again the system will be used to collect and store data from the model during the test for manipulation after a series of tests.

Appendix 1

Sensor Description

Sensor ID : GATANGLE

Scale (1-6) : 4
Mode (1-7) : 3

Sensor Description: ANGLE MEASUREMENT

Engineering Units (tag) : DEGREES

Calibrating Formula Values - (e.g., 6.25 mV -> 0.937 g)

60.0 mVolts / 1.007 Units

Data Conversion Coefficients - Date: 10-14-86 Calibration Flag : T

Values: +0000000000 x ^{4} +0000000000 x ^{3} +0000000000 x ^{2} +5.5944E-04 x +0000000000

Range :+17.90208 /-17.90208 Resolution :+5.5944E-04

F7=Special Keys F9=HELP F8=EXIT (Abort) F6=Calculate F10=END (accept)

OPTIM USERS' SOFTWARE TRANSDUCER LIBRARY SENSOR ENTRY

Sensor ID : GA LVDT SN98 Scale (1-6) : 6
Mode (1-7) : 1

Sensor Description: LVDT SN98 NO.3

Engineering Units (tag) : MM

Calibrating Formula Values - (e.g., 6.25 mV -> 0.937 g)

46.45 mVolts / 1 Units

Data Conversion Coefficients - Date: 07-03-87 Calibration Flag : T

$$\text{Values: } +0000000000 \times^{4} +0000000000 \times^{3} +0000000000 \times^{2} +7.1761E-03 \times +0000000000$$

Range :+229.6352 /-229.6352 Resolution :+.0071761

F7=Special Keys F9=HELP F8=EXIT (Abort) F6=Calculate F10=END (accept)

OPTIM USERS' SOFTWARE TRANSDUCER LIBRARY SENSOR ENTRY

Sensor ID : GA LVDT SN00 Scale (1-6) : 6
Mode (1-7) : 1

Sensor Description: LVDT SN00 NO.4

Engineering Units (tag) : MM

Calibrating Formula Values - (e.g., 6.25 mV -> 0.937 g)

46.45 mVolts / 1 Units

Data Conversion Coefficients - Date: 07-03-87 Calibration Flag : T

$$\text{Values: } +0000000000 \times^{4} +0000000000 \times^{3} +0000000000 \times^{2} +7.1761E-03 \times +0000000000$$

Range :+229.6352 /-229.6352 Resolution :+.0071761

F7=Special Keys F9=HELP F8=EXIT (Abort) F6=Calculate F10=END (accept)

Sensor ID : GA_LOAD_200K ← Scale (1-6) : 1

Mode (1-7) : 1

Sensor Description: LOAD CELL 200 KIPS

Engineering Units (tag) : LBS

Calibrating Formula Values - (e.g., 6.25 mV -> 0.937 g)

.000114 mVolts / 1 Units

Data Conversion Coefficients - Date: 12-11-86 Calibration Flag : T

Values: $+0000000000 \times^{4} +0000000000 \times^{3} +0000000000 \times^{2} +8.77193 \times -14400.000$

Range :+266301.8 /-295101.8 Resolution :+8.771484

F7=Special Keys F9=HELP F8=EXIT (Abort) F6=Calculate F10=END (accept)

OPTIM USERS' SOFTWARE TRANSDUCER LIBRARY SENSOR ENTRY

```
OPTIM  USERS' SOFTWARE                TRANSDUCER  LIBRARY  SENSOR  ENTRY

Sensor ID : SG120-CONC                          Scale (1-6)           : 1
                                                Mode (1-7)            : 3
Sensor Description:  STRAIN GAUGE 120OHMS       Excitation Type (A)   : A
                                                Excitation Value (mA) : 13.04
Engineering Units (tag) : MICROSTRAIN

Calibrating Formula Values -  (e.g., 1 arm, 120 ohms, +0.02 %, GF=1.80)

   Number of Active Bridge Arms : 1       Gage Resistance (ohms) : 120

   Transverse Sensitivity (%) : 1         Gage Factor : 2.06

Data Conversion Coefficients - Date: 06-16-87   Calibration Flag : T

                      4                3                2
Values: +0000000000 x +0000000000 x +0000000000 x -.3142893   x +0000000000

Range :+10057.26  /-10057.26                  Resolution :+.3142893

 F7=Special Keys  F9=HELP  F8=EXIT (Abort)  F6=Calculate  F10=END (accept)

OPTIM  USERS' SOFTWARE                TRANSDUCER  LIBRARY  SENSOR  ENTRY

Sensor ID : SG120-STEEL                         Scale (1-6)           : 1
                                                Mode (1-7)            : 3
Sensor Description:  STRAIN GAUGE 120OHMS       Excitation Type (A)   : A
                                                Excitation Value (mA) : 13.04
Engineering Units (tag) : MICROSTRAIN

Calibrating Formula Values -  (e.g., 1 arm, 120 ohms, +0.02 %, GF=1.80)

   Number of Active Bridge Arms : 1       Gage Resistance (ohms) : 120

   Transverse Sensitivity (%) : 1         Gage Factor : 2.04

Data Conversion Coefficients - Date: 06-16-87   Calibration Flag : T

                      4                3                2
Values: +0000000000 x +0000000000 x +0000000000 x -.3173705   x +0000000000

Range :+10155.86  /-10155.86                  Resolution :+.3173705

     Check Range & Resolution     F8=Resume Editing     F10=Accept,To Menu

OPTIM  USERS' SOFTWARE                TRANSDUCER  LIBRARY  SENSOR  ENTRY
```

Experiment Table

OPTIM USERS' SOFTWARE TRANSDUCER LIBRARY SENSOR ENTRY

Sensor ID : SG120-CONC-B

Scale (1-6) : 1
Mode (1-7) : 3
Excitation Type (A) : A
Excitation Value (mA) : 13.04

Sensor Description: STRAIN GAUGE 120OHMS

Engineering Units (tag) : MICROSTRAIN

Calibrating Formula Values - (e.g., 1 arm, 120 ohms, +0.02 %, GF=1.80)

Number of Active Bridge Arms : 1 Gage Resistance (ohms) : 120

Transverse Sensitivity (%) : 1 Gage Factor : 2.13

Data Conversion Coefficients - Date: 06-17-87 Calibration Flag : T

$$\text{Values: } +0000000000 \times +0000000000 \times^{4} +0000000000 \times^{3} -.3039605 \times^{2} +0000000000$$

Range :+9726.736 /-9726.736 Resolution :+.3039605

F7=Special Keys F9=HELP F8=EXIT (Abort) F6=Calculate F10=END (accept)

OPTIM USERS' SOFTWARE EXPERIMENT TABLE DATA ENTRIES

Experiment Date : 06-16-87 File : FLEX-1

Experiment Descr : FLEXURE-1 WSM

Run Description : TEST

Codes:
0=immediate
1=console
2=at HHMM
3=now+HHMM
4=on limits
5=rel.limit

Parameters:
OHHMM
OOccc

Start Code : 1 Stop Code : 1

Start Parameter : Stop Parameter :

Pre-trigger Count : 0 Limit Counter 1 : Limit Counter 2 :

Repeat Code (0-65535) : 200

Scan Interval in Seconds (0=continuous scanning) : 0

High or Low Speed Data Storage (L=immediate;H=when buffer full) : H

Data File Suffix : D12 Number of Channel Entries 19 & Pseudo Sensors 0

F7=Special Keys F9=HELP F8=Abort F10=Accept,Continue

OPTIM USERS' SOFTWARE EXPERIMENT TABLE CHANNEL ENTRIES

File: FLEX-1

Entry Numb.	Chan. Numb.	Sensor ID	Description	Balance Code	Balance Pattern	Limits High	Limits Low	Display
1	0	SG120-STEEL	TOP STEEL 1	2	+06322	3000	-3000	Y
2	1	SG120-STEEL	TOP STEEL 2	2	+06707	3000	-3000	Y
3	2	SG120-STEEL	TOP STELL 3	2	+05596	3000	-3000	Y
4	3	SG120-STEEL	BOTTOM STEEL 1	2	+09563	3000	-3000	Y
5	4	SG120-STEEL	BOTTOM STEEL 2	2	+11170	3000	-3000	Y
6	5	SG120-CONC	TOP CONCRETE 2	2	+10878	3000	-3000	Y
7	6	SG120-CONC	TOP CONCRETE 3	2	+09981	3000	-3000	Y
8	7	SG120-CONC	TOP CONCRETE 4	2	+13378	3000	-3000	Y
9	8	SG120-CONC-B	BOTTOM CONCRETE 1	2	+08345	3000	-3000	Y
10	9	SG120-CONC-B	BOTTOM CONCRETE 2	2	+08137	3000	-3000	Y
11	10	SG120-CONC-B	BOTTOM CONCRETE 3	2	+05524	3000	-3000	Y
12	11	SG120-CONC-B	BOTTOM CONCRETE 4	2	+06144	3000	-3000	Y
13	12	SG120-STEEL	BOTTOM STEEL 3	2	-00001	3000	-3000	Y
14	13	SG120-STEEL	BOTTOM STEEL 4	2	-00001	3000	-3000	Y
15	14	SG120-CONC	TOP CONCRETE 1	2	+05221	3000	-3000	Y

F6=Save Table (i.e., don't change the rest)
F3=Insert Line F4=Delete Line F7=Special Keys F9=HELP F8=Abort F10=Accept,Cont

OPTIM USERS' SOFTWARE EXPERIMENT TABLE CHANNEL ENTRIES

File : FLEX-1

Entry Numb.	Chan. Numb.	Sensor ID	Description	Balance Code	Balance Pattern	Limits High	Limits Low	Display
16	15	GA LOAD 200K	LOAD CELL - LBS	2	+02013	70000	0	Y
17	30	GA LVDT SN91	DEFLECTION 1 - MM	2	+32664	18	0	Y
18	32	GA LVDT SN92	DEFLECTION 2 - MM	2	+32763	18	0	Y
19	34	GA ANGLE	ANGLE - DEGREES	2	-30967	.5	0	Y
20								
21								
22								
23								
24								
25								
26								
27								
28								
29								
30								

End of Input Data F10=Screen Full,Add More Channels to End
F3=Insert Line F4=Delete Line F7=Special Keys F9=HELP F8=Abort F5=SAVE,To Menu

12-02-87 09:24:36

OPTIM USERS' SOFTWARE EXPERIMENT TABLE DATA ENTRIES

```
Experiment Date  : 09-25-87    File : TEST.E01      Number of Scans : -1
Experiment Descr :
Run Description  :                                  Starting Time : 12:08:42
                                                    Starting Date : 09-25-87
CMOS Table Entry :                                  Ending Time : 12:08:59
Use Auto-Balancing Values : Y                       Ending Date : 09-25-87

Start Code : 5              Stop Code : 5           Override with Console : *N
Start Parameter :           Stop Parameter :
Pre-trigger Count :         Limit Counter 1 :       Limit Counter 2 :

     Auto Tape Mark : Y
     Scan Entry to be Monitored thru A :        B :         C :

     Repeat Code (0-65535) : 0          Scan Mode : 1   (0=interval; 1=burst)

     OPUS Scan Interval in Seconds (0=continuous scanning) : 0
     MEGADAC Clock Type : 0   (0=internal;1=external)
             Clock Mode : 0   (0=samp/sec;1=sec/samp)    Clock Rate : 100

Data File Suffix : D01    Number of Channel Entries 4    & Pseudo Sensors 2
```

**END **

12-02-87 09:25:55

OPTIM USERS' SOFTWARE EXPERIMENT TABLE CHANNEL ENTRIES

File : TEST.E01

Entry Numb.	Chan. Numb.	Sensor ID	Description	Balance Code	Balance Pattern	Limits High, Low	Displa
1	048	SG350-TEST		2	+01394		Y
2	064	LC50K		2	-00994		Y
3	065	LC100K		2	-00525		Y
4	066	GALVDT-SN98		2	+00402		Y
5		%TIME-REL	MINUTES	0	+00000		Y
6		=E5*60	SECONDS	0	+00000		Y
7							
8							
9							
10							
11							
12							
13							
14							
15							

**END **

Transducer Calibration

```
 OPTIM  USERS' SOFTWARE                                CALIBRATE  TRANSDUCER
 1.  If NO autobalance is desired, go directly to Step 2.
     Set STEP to 1; set transducer on channel 029 to value 0; press F10.
     (MEGADAC will balance and give average of 10 readings.)
 2.  Set STEP to 2; set Actual Value to correct value; set transducer on
     channel 029 to the selected value; press F10.
     (MEGADAC will give average of 10 readings.)
 3.  Set STEP to 3; set Actual Value to correct value; set transducer on
     channel 029 to the selected value; press F10.
     (MEGADAC will give average of 10 readings & compute new coefficients.)
 4.  Set STEP to 4; set Actual Value to correct value; set transducer on
     channel 029 to the selected value; press F10.
     (MEGADAC will give average of 10 readings & compute percentage of error.)
 5.  Set STEP to 5; press F10 to accept new coefficients.
     WARNING: the new mX + b will replace all 5 of the previous coefficients.
Note: at any time you can abort (keep previous values) or start over with Step
                      Step 1          Step 2         Step 3         Step 4
  STEP: 5                      Percentage of Error:   1.2 %
  Actual Values:          0            -12.7          -25.4          -50.8
  Measured Values:   0.0000E+00     -.2440E+04     -.4881E+04     -.9878E+04
                     X^4            X^3            X^2            X
  previous: +0000000000  +0000000000  +0000000000  +7.1761E-03  +0000000000
  new            +0             +0             +0          +5.2038E-03  -2.0812E-03
  new ranges & resolution:  +156.1119   / -156.1161     +5.2038E-03
                         F8=Abort        F10=Accept
```

```
 OPTIM  USERS' SOFTWARE                                CALIBRATE  TRANSDUCER
 1.  If NO autobalance is desired, go directly to Step 2.
     Set STEP to 1; set transducer on channel 029 to value 0; press F10.
     (MEGADAC will balance and give average of 10 readings.)
 2.  Set STEP to 2; set Actual Value to correct value; set transducer on
     channel 029 to the selected value; press F10.
     (MEGADAC will give average of 10 readings.)
 3.  Set STEP to 3; set Actual Value to correct value; set transducer on
     channel 029 to the selected value; press F10.
     (MEGADAC will give average of 10 readings & compute new coefficients.)
 4.  Set STEP to 4; set Actual Value to correct value; set transducer on
     channel 029 to the selected value; press F10.
     (MEGADAC will give average of 10 readings & compute percentage of error.)
 5.  Set STEP to 5; press F10 to accept new coefficients.
     WARNING: the new mX + b will replace all 5 of the previous coefficients.
Note: at any time you can abort (keep previous values) or start over with Step
                      Step 1          Step 2         Step 3         Step 4
  STEP: 5                      Percentage of Error:   0.8 %
  Actual Values:          0            -12.7          -25.4          -50.8
  Measured Values:   0.5120E+03     -.1782E+04     -.4161E+04     -.8882E+04
                     X^4            X^3            X^2            X
  previous: +0000000000  +0000000000  +0000000000  +5.7361E-03  -2.828586
  new            +0             +0             +0          +5.7401E-03  -2.191475
  new ranges & resolution:  +157.0217   / -157.3847     +5.7401E-03
                         F8=Abort        F10=Accept
```

Measurements

```
*** Sample Number 2 ***
1       048    SG350-TEST                          MICROSTRAIN    0
2       064    LC50K                               lbs            0
3       065    LC100K                              lbs            0
4       066    GALVDT-SN98                         MM             0
5              %TIME-REL      MINUTES              *****          0
6              =E5*60         SECONDS              *****          0


*** Sample Number 19 ***
1       048    SG350-TEST                          MICROSTRAIN    0
2       064    LC50K                               lbs            0
3       065    LC100K                              lbs            0
4       066    GALVDT-SN98                         MM             0
5              %TIME-REL      MINUTES              *****          0
6              =E5*60         SECONDS              *****          0


  OPTIM  USERS' SOFTWARE                    LISTING  OF  MEASURED  RESULTS

                    DIRECTORY OF .Enn and .Dnn FILES
------------ ------------ ------------ ------------ ------------ ------------

CDR1000.ED1                           CDR1000.EDF
TEST.E01                              UM.E01
FLEX-1.E01                            TEST.E02

OPUSMODE.DEF                          XMITSPC.DEF
FLEX-1.D01                            TEST.D01


          Shift/PrtSc=Print                    F10=Continue
```

Appendix 2

Centrifuge Modelling of Explosion Induced Craters

Carlos H. Serrano
Richard D. Dick
Deborah J. Goodings
William L. Fourney
University of Maryland, College Park MD 20742 USA

ABSTRACT: Thirty-three 1gm cylindrical charges of PETN with lead azide as an initiator were half-buried in dry sand and detonated on the centrifuge at accelerations varying between 1g and 100g. The volumes of the craters varied as $g^{-0.450}$ or in terms of extrapolated prototype volumes and prototype charge weights, as $W^{0.850}$. This latter relationship is in very good agreement with research by Schmidt and Holsapple (1980) who worked predominantly at accelerations greater than 300g. Absolute magnitudes of prototype craters predicted by the two works differ, however; it is speculated that this may be due to differences in soil unit weight and charge geometry. Neither work is successful in predicting the volumes of four selected field craters, although they are considered to be close enough to confirm in general the validity of the technique.

1 INTRODUCTION

Many parameters describing soils and explosives affect the size of an explosion induced crater of which charge weight ,W, is one of the most easily varied. Analysis of the effect of changes in W has been undertaken by several authors. This has included, for example, an evaluation by Chabai (1965) of theoretical work, an analysis of field data by Rooke et al. (1974) and a comparison of theory to a statistical analysis of field data by Dillon (1972). They proposed that the volume of the apparent crater (that which is defined by the hole left in the ground caused by the detonation of the explosive, rather than the limits of plastic deformation of the underlying soil) is a function of W^n where n is an exponent predicted to lie between 0.75 and 1.00.

The fact that a value for n has not been fixed within a smaller range is, in part, a product of enormous scatter in field data. Such data has often been characterized by either incorrect records or missing geotechnical data. Further, attempts have been made to compare the craters from quite different explosives with fundamental and unquantified differences in character, or the craters produced in quite different geotechnical conditions. This unsatisfactory definition of a value for n led to the use of physical models. The most successful technique which best satisfies the requirements for similarity has involved the use of the geotechnical centrifuge.

The best systematic and readily available set of data for the simple case of craters produced on the centrifuge by half-buried charges in dry sand has been reported by Schmidt and Holsapple (1980) who worked at low accelerations (10g) and high (306g, 451g and 463g). They also incorporated into their work results from nine laboratory tests at 1g by Piekutowski (1974). They were satisfied with their tests from the two points of view of repeatability and modelling of a single hypothetical crater at different scales.

Most geotechnical centrifuges, however, are operated at accelerations much lower than 306g but still higher than 10g. The purpose of this research, then, was to examine two questions: whether the trends in modelling crater development observed by Piekutowsky at 1g, and by Schmidt and Holsapple at 10g and above 300g are also observed at accelerations of 100g and below; and whether field data confirms the correctness of extrapolation from models to full scale explosions in this range of scales.

Dillon, L.A., 1972, The Influence of Soil and Rock Properties on the Dimensions of Explosion-Produced Craters, U.S. Air Force Weapons Laboratory, Technical Report 891 964.

Haskell, N.A., 1955, Some Considerations on the Modelling of Crater Phenomena in Earth, Air Force Survey of Geophysics, No. 67, TN-55-205, Air Force Cambridge Research Center, Bedford, MA.

Lampson, C.W., 1946, Explosions in Earth, In Effects of Impact and Explosion Vol 1, Office of Research and Development, Washington, D.C.

Ovesen, N.K., 1979, The Scaling Law Relationship, Panel Discussion, Proc. 7th European Conference on Soil Mechanics, Vol. 4: 319-323.

Piekutowsky, A.J., 1974, Laboratory-Scale High-Explosive Cratering and Ejecta Phenomenology Studies, Air Force Weapons Laboratory, Technical Report 783 622.

Rooke, A.D., Carnes, B.L., and Davis, L.K., 1974, Cratering by Explosions: A Compendium and an Analysis, U.S. Army Engineers Waterways Experiment Station, Technical Report B024 657.

Sachs, R.G., 1944, Dependence of Blast on Ambient Pressure and Temperature, Report BRL-466, Ballistic Research Laboratory, Aberdeen MD.

Schmidt, R.M., and Holsapple, K.A., 1980, Theory and Experiments on Centrifuge Cratering, Journal of Geophysical Research, Vol. 85, No. B1, pp. 235-252.

Serrano, C.H., 1987, A Check for Scaling Effects on Explosion Induced Craters-Centrifuge Model Testing, M.S. Thesis, University of Maryland.

that the data line of this research consistently overestimates crater size, as does Schmidt and Holsapple's data line in three out of four cases, although to a lesser degree. Failure of the centrifuge models to predict more closely the sizes of the prototype craters may be attributed to a combination of unquantifiable differences in the explosives used, unidentified differences in the soils, and other unexplained reasons responsible for the field scatter, some of which are considered below. But in the absence of more care in field control and documentation to narrow the scatter of full scale data, the closeness of the research data lines to the field data points in Figure 2 is considered to be a general confirmation of the modelling technique.

Figure 2 also highlights the fact that Schmidt and Holsapple's data line is not coincident with the data line from this research, even when the same soil and explosive were used. It is speculated that this may be a result of small differences in soil unit weight: their values of γ_d were on average 5% greater than for this research. This was not a parameter conclusively assessed quantitatively for its influence on crater size by either study, but it is known qualitatively from other tests by Serrano that explosives detonated in a loosely packed soil will produce craters larger than those in the same soil more densely packed. Unrecorded differences in soil unit weights for the field tests may account in part for the fact that they lie below the two research data lines. The difference may also be a function of charge geometry.

Although the centres of gravity of all the charges were at the soil surface, it seems reasonable to assume that the half of the charge below the soil surface will have a greater influence on the development of a crater than the half above the soil surface. The geometry of a horizontal cylindrical charge with an aspect ratio of one is such that the centre of gravity of the buried half is slightly deeper than the centre of gravity of the buried half of a sphere. It is known that for depths less than the optimum depth of burial the crater size increases with depth. It is possible to speculate, then, that this difference in geometry has the effect that the half-buried cylindrical charge will produce a larger crater than Schmidt and Holsapple's half-buried spherical charge, although this alone is not considered sufficient to explain the difference in crater volumes seen on Figure 2. This geometry effect would be exaggerated by differences in charge density. Certainly this effect is not considered in field tests and may explain some field data scatter.

4 CONCLUSIONS

The relationship between prototype weights of explosives and prototype crater volumes for half-buried charges in sand developed by Schmidt and Holsapple from centrifuge tests at accelerations predominantly greater than 300 g was confirmed by thirty-three models tested at less than 100g for this research; while the relationships fell in the midst of those developed both theoretically, and empirically from field data of widely varying explosive and field conditions, they did not agree with any. Comparison of test results to data of crater sizes from a small set of field tests selected because field conditions and sizes of explosives seemed close to those modelled, showed that this research overpredicted field crater size, and Schmidt and Holsapple's tended also to do the same, although to a lesser degree. This is attributed to unquantified differences in field conditions. The closeness of the points to the research data lines is interpretted as a general confirmation of the validity of the technique. The discrepancy between actual crater sizes predicted by Schmidt and Holsapple compared to those of this research is attributed to effects arising from differences in sand densities and charge geometries.

ACKNOWLEDGMENT

This research was carried out under grant number 86-0095 from the U.S. Air Force Office of Scientific Research. The authors are grateful for the support and encouragement from that office. They are also grateful for advice from Dr. R.M. Schmidt.

REFERENCES

Chabai, A.J., 1965, On Scaling Dimensions of Craters Produced by Buried Explosives, Journal of Geophysical Research, Vol. 70, No. 20: 5075-5098.

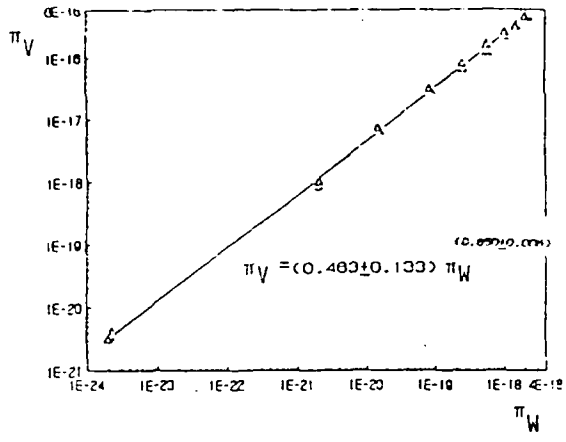

Figure 1 - π_W vs π_V

analyze the results included:

$$\pi_V = V(g/Q_e)^3 \qquad (1)$$

$$\pi_R = Rg/Q_e \qquad (2)$$

$$\pi_H = Hg/Q_e \qquad (3)$$

$$\pi_W = (W/\delta)(g/Q_e)^3 \qquad (4)$$

where V is apparent crater volume, R is apparent crater radius, H is apparent crater depth measuring from the elevation of the original soil surface to the maximum depth of the crater, g is gravitational acceleration at the time of detonation, Q_e is specific energy (6.75×10^{10} ergs/gm for this explosive), δ is charge density (varying between 1.46 and 1.56 gm/cm^3 in twenty-eight tests, 1.39 gm/cm^3 in four tests, and 1.65 gm/cm^3 in one test) and W is charge weight. These are rearrangements of π groups developed by Schmidt and Holsapple. Since the effects of neither soil nor explosive properties on crater formation were specifically examined, by using the same soil and explosive in all cases, any π groups involving characteristics of the soil or the explosive exclusively are not included in this presentation although Serrano does give attention to them.

Because the characteristics of the charge are reflected in the π_W group, π_V, π_R and π_H were analyzed as functions of π_W. Figure 1 shows a logarithmic plot of the data of π_W and π_V. The best least squares fit between the two π groups is shown on that figure as:

$$\pi_V = (0.463 \pm 0.133)\ \pi_W^{(0.850 \pm 0.005)} \qquad (5)$$

for an arbitrarily selected 80% confidence interval. Similar fits for π_R and π_H are not plotted here but the relationships are:

$$\pi_R = (1.341 \pm 0.137)\ \pi_W^{(0.288 \pm 0.003)} \qquad (6)$$

and

$$\pi_H = (0.086 \pm 0.017)\ \pi_W^{(0.257 \pm 0.004)} \qquad (7)$$

In terms of relating these π relationships to the experiments, where all parameters are constant but g, they can be manipulated to relate apparent model crater dimensions to acceleration as:

$$V \alpha g^{-0.450 \pm 0.015} \qquad (8)$$

$$R \alpha g^{-0.136 \pm 0.009} \qquad (9)$$

$$H \alpha g^{-0.229 \pm 0.012} \qquad (10)$$

or in extrapolating to full scale tests where g is constant but explosive weight, W, is varied:

$$V \alpha W^{0.850 \pm 0.005} \qquad (11)$$

$$R \alpha W^{0.288 \pm 0.003} \qquad (12)$$

and $$H \alpha W^{0.257 \pm 0.004} \qquad (13)$$

If craters are assumed to be approximately parabolic with a constant shape, then the sum of twice the radius exponent plus the height exponent for W in equations 12 and 13 should equal the exponent for W in equation 11. This expectation is satisfied well here: $2(0.288) + 0.257 = 0.833$ which is less than 0.850 by 2%.

3.2 Comparison with Other Analyses

Although the radius and the depth of a crater are important measures of cratering efficiency, let us focus on crater volume alone for comparison to the findings of other researchers. The consensus of researchers, also confirmed here, is that crater volume is exponentially dependent on charge weight, in the form of:

$$V \propto W^n \qquad (14)$$

but there is significant divergence on what the value of that exponent n should be.

Chabai (1965) cited theoretical work of Sachs (1944) and Lampson (1946) both of whom concluded with values of n=1.0, and Haskell (1955) who concluded with a value of n=0.75; but Chabai then dismissed these values as being unsound from the two

2 METHOD

Forty-two models were prepared for the research. The sand used to form the bed for the explosive and the cratering medium was a dry, uniformly graded, Flintshot 2.8 Sawing-Trap quartz Ottawa sand with D_{50} = 0.6 mm and C_u = 1.31, the same as that used in six of Schmidt and Holsapple's ten tests. The sand was rained into a 475 mm diameter 400 mm deep aluminum test container from a height of 0.70 m to achieve a unit weight of 16.72 kN/m^3 ± 0.03, or a void ratio of 0.555 ± 0.003. In thirty-two models, the completed depth of the sand bed was 254 mm. In ten models sand bed depth effects were examined, varying the depth from 360 mm to 102 mm.

The explosive used was 1gm of PETN (Pentaerythritol-tetranitrate) selected based on the experience of Schmidt and Holsapple. It was packed at an average density of 1.5 gm/cm^3 into a cylindrical form with diameter of 9.6 mm and height varying from 8.9 mm to 10.0 mm to give an aspect ratio as close as possible to 1.0. Lead azide was used as the initiator because it is much less stable than PETN, although its specific energy is less. The combined energy released by the two together is calculated to be the equivalent of 1.005 gm of PETN or 1.397 gm of TNT. The finished charge was pressed into the sand bed to a half-buried position with the longitudinal axis of the cylinder placed horizontally.

Models were accelerated on the 200g 30,000g-lb Genisco centrifuge to the desired acceleration, the explosion was detonated, and the centrifuge was slowed after the video camera picture of the model indicated the dust had settled and the gases had dispersed. The dimensions of the crater were recorded measuring across four complete diameters using a simple profilometer which measures vertical distance to the soil surface from the horizontal datum defined by the top of the centrifuge model test container. These eight radii were used to calculate an average half crater profile from which crater volume was in turn calculated by means of cylindrical shells. Contour maps could also be produced from the profilometer data.

Of the forty-two models tested, the results of five were discarded due to known experimental error, and four were discarded because of small but detectable boundary effects in models with sand beds less than 178 mm. The coefficient of variation at any single acceleration for the remaining thirty-three tested was no more than 15%, which is considered to be quite acceptable. The data of the remaining models is given in Table 1.

Table 1. Model Test Data.

Gravity [g]	Test No.	Sandbed Thickness [cm]	Crater Volume V_3 [cm^3]	Crater Radius R [cm]	Crater Depth D [cm]
1	11	30.48	1,136.0	13.49	4.3
	12	25.40	1,392.0	14.24	5.5
	31	25.40	1,038.6	14.02	4.9
10	29	25.40	347.7	9.13	2.4
	30	25.40	287.2	9.07	2.4
20	10	25.40	307.7	8.86	2.6
	23	25.40	275.8	8.90	2.3
	38	25.40	273.8	8.90	2.3
	39	25.40	253.8	8.13	2.3
35	16	25.40	237.1	8.43	2.3
	18	25.40	220.7	8.53	2.3
	24	25.40	238.0	7.93	2.3
	46	25.40	231.9	8.27	2.3
	47	25.40	216.2	8.00	2.2
50	17	25.40	208.3	7.87	2.2
	19	25.40	187.0	7.83	1.9
	25	25.40	169.4	7.63	1.8
65	13	25.40	161.8	7.25	1.8
	15	25.40	138.7	7.44	1.8
	20	25.40	189.8	7.80	1.9
	26	25.40	186.0	7.74	2.0
	42	30.48	173.3	7.63	1.9
	43	30.48	143.7	7.94	1.7
	44	17.78	187.6	7.81	1.8
80	21	25.40	161.0	7.88	1.7
	27	25.40	158.7	7.56	1.7
	28	25.40	141.4	7.55	1.6
90	22	25.40	147.6	7.46	1.7
	32	25.40	137.1	7.38	1.7
	34	25.40	145.8	7.40	1.7
100	14	25.40	142.6	7.29	1.7
	35	25.40	144.0	7.16	1.6
	45	17.78	146.2	7.48	1.6

3 DISCUSSION

3.1 Internal Trends

Ovesen (1979) emphasized the use of the Buckingham π dimensional analysis in geotechnical modelling, and Schmidt and Holsapple, too, have been strong advocates of this technique. The technique was also used here. Serrano (1987) defined a complete set of π groups to define these cratering events. The ones used to

END

DATE

FILMED

4-88

DTIC